Research Article

Formulation and characterization of SPIONs (Super Para-magnetic Iron Oxide Nanoparticles): A study on metal nanoparticles for drug delivery

Sameea Ahmed Khan

Department of Pharmaceutics, School of Pharmaceutical Education and Research, Jamia Hamdard, New Delhi

Abstract

Metal nanoparticles, especially iron oxide nanoparticles have mustered popularity owing to its unique properties over other nano- formulations/ nanocarriers. Due to its super- para magnetic nature, it is abbreviated as SPIONs (Super Paramagnetic Iron Oxide Nanoparticles). Superparamagnetic iron oxide nanoparticles (SPIONs) have received substantial interest owing to their potential applications in the fields of magnetic storage, catalysis, electro-catalysis and biomedical field, e.g., hyperthermia treatment, targeted drug delivery and contrast agents for magnetic resonance imaging (MRI). In this study, SPIONs were formulated and characterized for better understanding of the nano drug delivery systems. The development and characterization of SPIONs were conducted. Due to its nano- size, longer blood circulation time is possible and also, better absorption.

Keywords: nanoparticles, drug development, drug delivery, nanomedicine.

1. Introduction

The increasing interest for SPIONs is due to the discovery of their physical and chemical properties. In particular, it has been shown that the magnetic anisotropy of magnetic nanoparticles can be much greater than those of a bulk specimen, while differences in the Curie or Néel temperatures, i.e., the temperatures of spontaneous parallel or antiparallel orientation of spins between MNP and the corresponding microscopic phases, reach hundreds of degrees [1, 2]. In addition, magnetic nanomaterials have been found to possess a number of interesting properties such as giant magnetoresistance or abnormally high magneto caloric effect [3]. Coated and multiply derivatized super para- magnetic iron oxide nanoparticles for drug delivery systems have become the centre of research [4-6]. In the biomedical arena,

Research Article

nanoparticles are the subject of fast-moving developmental efforts in, e.g., diagnostic imaging [7, 8]. Super para- magnetic iron oxide nanoparticles (SPIONs) with a diameter of around 10 nm have been used for many years for, e.g., non- viral gene delivery, as MRI contrast agents, or for typical separation applications [9, 10]. It has been shown that magnetic particles are physiologically well tolerated and that the surface of the particles is responsible for the biocompatibility and stability to the reticuloendothelial system [11, 12]. In this context it is very important to realize that the size, usually in the 15 nm range, and the size distribution of the nanoparticles suitably modified for biocompatibility play a crucial in achieving the goals in the above applications [13, 14]. In particular as the particle size decreases the surface properties are dominated by the structural disorder at the surface which will affect the functionalization of the particles for a given application [15-17]. In this study, we will develop and characterize SPIONs and understand the importance of controlling these important physiochemical parameters for developing an efficient drug delivery system.

2. Materials and methods-

Ferric chloride anhydrous ($FeCl_3$) and ferrous sulphate heptahydrate ($FeSO_4.7H_2O$) were purchased from Thomas Baker Pvt. Ltd., India. Ammonia solution (25% v/v AR) and ammonium persulfate was purchased from s d fine- Chem. Ltd., India. All chemicals were of analytical grade and were used as purchased.

3. Formulation development-

3.1 Synthesis of SPIONs or pristine magnetite:

Ferrous Sulphate Heptahydrate and Ferric Chloride (anhydrous) were weighed in 2:1 ratio. They were both dissolved individually in distilled water and were subjected to magnetic stirring for about 20 minutes. A 2- neck flask was fitted in the clamp stand and placed in an oil/ sand bath to maintain a temperature of 60^0- 70^0 C. One neck was used to add solutions to the flask slowly while the other neck was fitted with nitrogen supply. 5 ml of 50% solution of conc. Ammonia was added dropwise. After all the compounds were added to the flask, it was heated and stirred simultaneously. A black coloured solution was formed at the end [18, 19].

The formulation was mixed with a lyoprotectant. It was then placed in the lyophilizer to obtain a powder form of the formulation. It was then stored in air- tight amber coloured containers for further use.

Research Article

3.2 Characterization of SPIONs:

3.2.1 Particle size measurement:

Particle size and zeta potential of the nanoparticles was measured by the standardized method. The samples were diluted with water and probe sonicated for 5 minutes at room temperature. Particle size was measured [20-22].

3.2.2 Zeta potential measurement:

The sample was diluted with distilled water. Zeta potential or the electrostatic repulsion between the particle and liquid medium was measured [23, 24].

3.2.3 Surface morphology by Transmission Electron Microscopy (TEM):

Morphology of SPIONs was seen by Transmission Electron Microscopy (TECNAI G^2 (220kV) HR- TEM; FEI). Appropriately diluted samples were negatively stained using the dye uranyl acetate and poured on the copper grid and dried to become thin films. The sample was placed in a vacuum chamber. The beam passes through them and this image was digitally recorded and observed [25-27].

3.2.4 X-ray Diffraction (XRD):

X-ray diffractometer (XRD) (Rigaku RAD-B system) was used to characterize the phase composition and crystallinity of the materials at a scanning rate of 3°/min, employing Cu Kα radiation (λ = 0.15405 nm) [28, 29].

3.3 Iron content assay:

2M hydrochloric acid solution was added to the formulation. The sample was treated with 2mg of ammonium persulfate and 1.5M of colouring agent potassium thiocyanate. 10 mL of an unknown sample solution was pipetted into a 250 mL volumetric flask and dilute to the mark with distilled water. The flask was shaken several times to mix the solution. 25 mL aliquots of this solution was added into 50 mL volumetric flask. The mixture was allowed to stand for 10 minutes. The flask was filled up to the mark with distilled water and mixed well by shaking the capped volumetric flask several times. Using the Spectronic 301

Research Article

spectrophotometer, the absorbance was measured. The quantitative determination of Fe^{3+} was done at λmax. 243 nm and that of Fe^{2+} at λmax. 245 nm [30-32].

4 Results and Discussion:

4.1 Formulation synthesis:

The co-precipitation technique is among the most simple and efficient synthesis procedures. It is based on simultaneous precipitation of Fe^{2+} and Fe^{3+} aqueous salt solutions via the addition of a weak or strong base [33]. Most of commercially available SPIONs are synthesized via this method. The co-precipitation technique is one of the most cost- effective routes for the high- yield synthesis of SPION with appropriate magnetic properties [34, 35]. Superparamagnetic iron oxide nanoparticles (SPIONs) were prepared by alkaline co-precipitation of ferric and ferrous chlorides in aqueous solution as described. Figure 1 shows that when the magnet was placed at a certain height near the test tube outside, the formulation moved upwards towards the magnet.

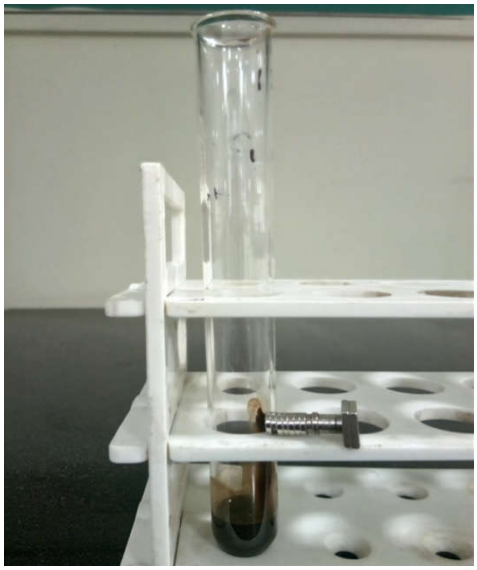

Figure 1: The magnet has caused the liquid formulation to move upwards in the test tube.

Research Article

4.2 CHARACTERIZATION OF NANOPARTICLES:

4.2.1 Particle size distribution:

The magnetic properties of nanoparticles depend on their size, shape and microstructure. The size of nanoparticles was found to be 273 nm with a polydispersity index (PDI) of 0.4. Figure 2 shows the graph for particle size measurement.

Figure 2: Particle size of SPIONs.

4.2.2 Zeta potential of SPIONs:

The zeta potential indicates the stability of ions in the solution. The zeta potential should ideally lie in the range of -30 mV to +30 mV. Here, the zeta potential was found to be -26 mV. Figure 3 shows the graph for zeta potential measurement.

Research Article

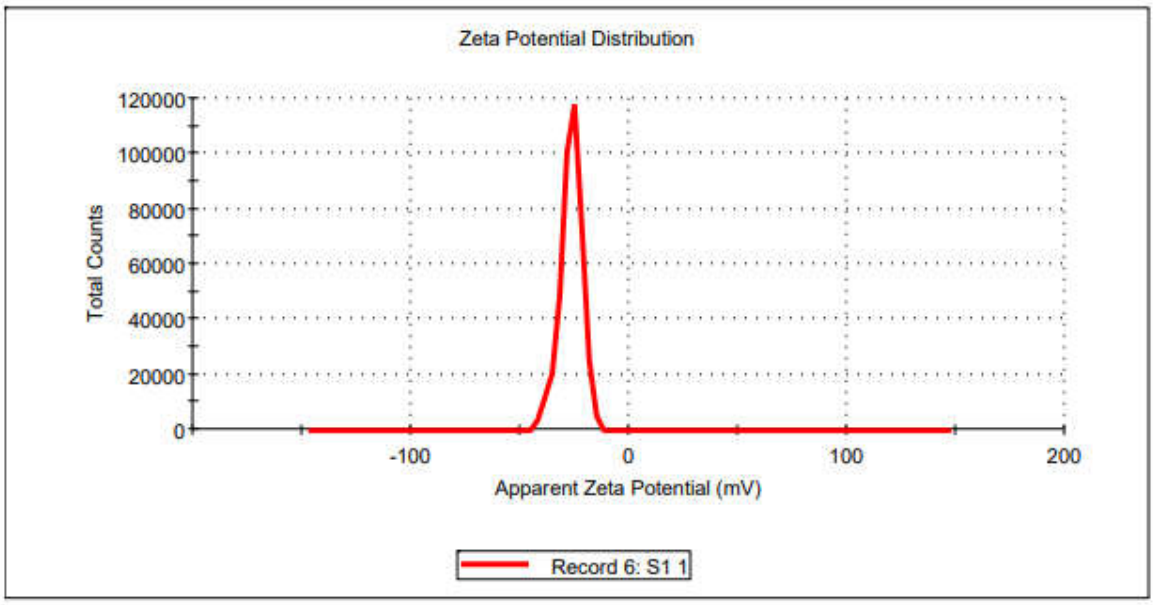

Figure 3: Zeta potential of SPIONs.

4.2.3 Particle shape (TEM)-

Figure 4 reveals the TEM photomicrographs. The shape of AA- SPIONs was found to be having spherical shape with monodispersed particles with the average size of 300 nm which is analogous to DLS measurements. Generally, TEM measures the particle size of static particles.

Figure 4: TEM image of SPIONS.

Research Article

4.2.4. X-ray Diffraction (XRD)

In order to identify the physical state and crystallinity, the XRD spectra of native Fe_3O_4 and XRD of formulation was carried out. The characteristic crystalline peaks at various 2θ positions of 10°, 13°, 17°, 21°, 26°, 30°, 35°, 39°, 44°, 50° and 53°, corresponding to *hkl* values of {131}, {151}, {168}, {182}, {148},{171}, {193}, {184}, {157}, {164} and {166}. This proved that there was no change in the crystallinity of the formulation.

4.3 Iron content assay-

Colorimetric analysis is based on the change in the intensity of the colour of a solution with variations in concentration. Colorimetric methods represent the simplest form of absorption analysis. An increase in sensitivity and accuracy results when a spectrophotometer is used to measure the colour intensity. Basically, it measures the fraction of an incident beam of light which is transmitted by a sample at a particular wavelength. To measure the difference in intensity of the light beam, percent absorbance is calculated. For any given compound, the amount of light absorbed depends upon (a) the concentration, (b) the path length, (c) the wavelength and (d) the solvent. Absorbance is related to the concentration according to the Beer-Lambert law:

$A = €bc$

Where € is the extinction coefficient (m^{-1} cm^{-1}), b is the solution path length (cm) and c is the concentration (moles $litre^{-1}$). The reaction between the iron (III) ion and the iso- thiocyanate ion takes place as follows:

$$Fe^{+3}(aq.) + 6SCN^{-}(aq.) \rightarrow [Fe(SCN)_6]^{3-}\ (aq.)$$

The iron content of SPION formulation was found to be 5.4% of Fe^{2+} and 4.63% of Fe^{3+}. Figure 5 shows the picture of the colorimetric estimation and calibration curves.

Research Article

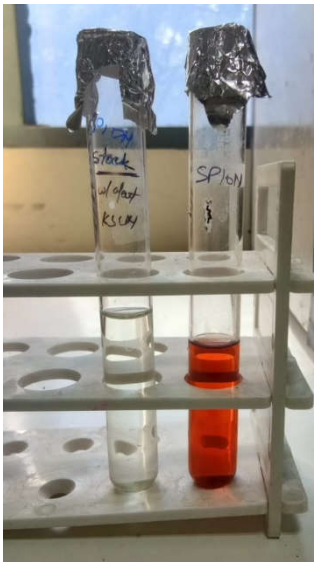

(A)

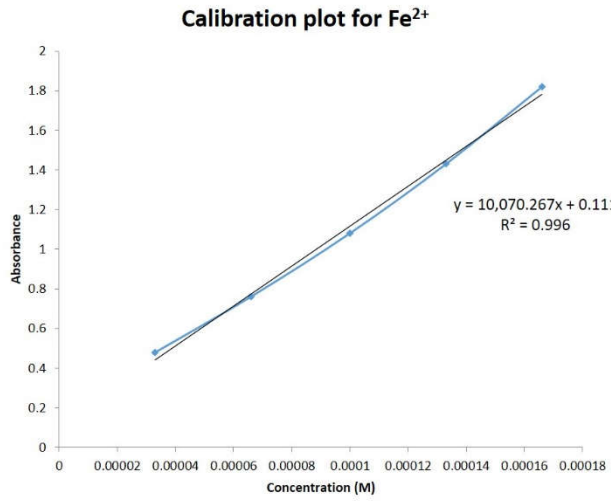

(B)

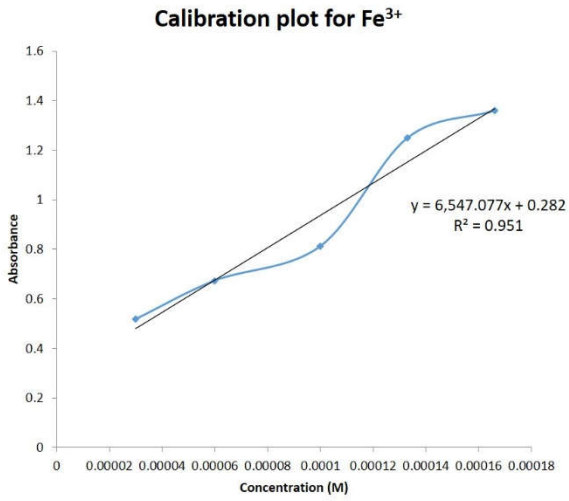

(C)

Figure 5: (A) Pictorial depiction of colorimetric reaction for Ferric and Ferrous estimation. (B) Calibration plot of Fe^{2+} ion and (C) Fe^{3+} ion

5. CONCLUSION:

In this study, SPIONs were formulated and characterized for better understanding of the nano drug delivery systems. The development and characterization of SPIONs were conducted. Various characterization techniques were used to understand the physicochemical properties

Research Article

of iron oxide nanoparticles. Due to its nano- size, longer blood circulation time and also, better absorption was observed. SPIONs form an important category of nano drug delivery in the current scenario. Magnetic fields and nanoparticles have been harnessed for therapy, diagnostics and drug delivery. It is concluded that this study can be further used to continue to improve the properties of magnetic particles and drug carriers, as well as developing technologies for cost-effective scale-up of magnetic systems.

6. REFERENCES:

1. https://www.nhlbi.nih.gov/siteindex
2. Al-Jamal, K. T., Bai, J., Wang, J. T.-W., Protti, A., Southern, P., Bogart, L., Pankhurst, Q. A. (2016). Magnetic drug targeting: Preclinical in vivo studies, mathematical modeling, and extrapolation to humans. Nano Letters, 16(9), 5652–5660.
3. Altanerova, U., Babincova, M., Babinec, P., Benejova, K., Jakubechova, J., Altanerova, V., Altaner, C. (2017). Human mesenchymal stem cellderived iron oxide exosomes allow targeted ablation of tumor cells via magnetic hyperthermia. International Journal of Nanomedicine, 12, 7923–7936.
4. Andrews, D. L., Lipson, R. H., & Nann, T. (2019). Comprehensive nanoscience and nanotechnology (Vol. 3, 2nd ed., pp. 193–210). Elsevier. Arami, H., Khandhar, A., Liggitt, D., & Krishnan, K. M. (2015). In vivo delivery, pharmacokinetics, biodistribution and toxicity of iron oxide nanoparticles. Chemical Society Reviews, 44(23), 8576–8607.
5. Blanco-Andujar, C., Ortega, D., Southern, P., Pankhurst, Q. A., & Thanh, N. T. K. (2015). High performance multi-core iron oxide nanoparticles for magnetic hyperthermia: Microwave synthesis, and the role of core-to-core interactions. Nanoscale, 7(5), 1768–1775.
6. Bobo, D., Robinson, K. J., Islam, J., Thurecht, K. J., & Corrie, S. R. (2016). Nanoparticle-based medicines: A review of FDA-approved materials and clinical trials to date. Pharmaceutical Research, 33(10), 2373–2387.
7. Boissenot, T., Bordat, A., Fattal, E., & Tsapis, N. (2016). Ultrasound-triggered drug delivery for cancer treatment using drug delivery systems: From theoretical considerations to practical applications. Journal of Controlled Release, 241, 144–163.

Research Article

8. Chen, Q., Zhang, S.Z., Ying, H.Z., Dai, X.Y., Li, X.X., Yu, C.H. and Ye, H.C., 2012. Chemical characterization and immunostimulatory effects of a polysaccharide from Polygoni Multiflori Radix Praeparata in cyclophosphamide-induced anemic mice. *Carbohydrate Polymers*, *88*(4), pp.1476-1482.
9. Ludwig H, Mu¨ldu¨ r E, Endler G, Hu¨bl W, 2013. Prevalence of iron deficiency across different tumors and its association with poor performance status, disease status and anaemia. Ann Oncol; 24; 1886–92.
10. Thurnham DI, McCabe LD, Haldar S, 2010. Adjusting plasma ferritin concentrations to remove the effects of subclinical inflammation in the assessment of iron deficiency: a meta-analysis. Am J Clin Nutr; 92:546–55.
11. Kovesdy CP, Estrada W, Ahmadzadeh S, Kalantar-Zadeh K, 2009; Association of markers of iron stores with outcomes in patients with nondialysis- dependent chronic kidney disease. Clin J Am Soc Nephrol; 4:435–41.
12. McClung J, Murray-Kolb L, 2013. Iron nutrition and premenopausal women: Effects of poor iron status on physical and neuropsychological performance. Annu Rev Nutr; 33:271–288.
13. Silber M, Becker P, Earley C, 2013. Willis- Ekbom Disease Foundation revised consensus statement on the management of restless legs syndrome. Mayo Clin Proc; 88:977–986.
14. Chandrasekharan, P.; Maity, D.; Yong, C. X.; Chuang, K. H.; Ding, J.; and Feng, S. S., Biomaterials, 2011, 32, 5663. **DOI:** 10.1016/j.biomaterials.2011.04.037
15. Birgit T., Olivares M., Héctor C., 2004. Enhancers of Iron Absorption: Ascorbic Acid and other Organic Acids. Int. J. Vitam. Nutr. Res. Hogrefe & Huber Publishers; 74 (6).
16. Beshara S, Lundqvist H, Sundin J, et al. 1999. Kinetic analysis of Fe labeled iron sucrose. Br. J. Hematol.; 104:288-95.
17. Abbasi, A.Z., 2011. Magnetic capsules for NMR imaging: effect of magnetic nanoparticles spatial distribution and aggregation. J. Phys. Chem. C. ACS Publications; 115 (14), 6257_6264. Smolensky E, J. Mater, 2013. Chem. B 1 (22).
18. Zhang J., 2014., Pharm. Res. 31 (3) 579.
19. Naha P. C, 2014, J. Mater. Chem. B 2 (46) 8239.

Research Article

20. Auerbach M, Strauss W, Auerbach S, 2013. Safety and efficacy of total dose infusion of 1020 mg ferumoxytol administered over 15 minutes. Am J Hematol; 88:944–947.
21. Chertow G, Mason P, Vaage-Nilsen O, 2006. Update on adverse drug events associated with parenteral iron. Nephrol Dial Transplant; 21:378–382.
22. West AR, Oates PS, 2008. Mechanisms of heme iron absorption: current questions and controversies. World J Gastroenterol.; 14: 4101-4110.
23. Ganz T., 2005. Hepcidin — a regulator of intestinal iron absorption and iron recycling by macrophages. Best Pract Res Clin Haematol; 18: 171- 182.
24. Laurent S, Forge, Port M, Roch A, Robic C, et al., 2008. Magnetic Iron Oxide Nanoparticles: Synthesis, Stabilization, Vectorization, Physicochemical Characterizations, and Biological Applications. Chem. Rev.; 108, 2064–2110.
25. Jain, T. K.; Morales, M. A.; Sahoo, S. K.; Leslie-Pelecky, D. L.; Labhasetwar, V., 2005. Mol. Pharm.; 2 (3), 194.
26. Chourpa, I.; Douziech-Eyrolles, L.; Ngaboni-Okassa, L.; Fouquenet, J. F.; Cohen-Jonathan, S.et al. 2005. Analyst; 130 (10), 1395.
27. Ai, H., 2003. Nano-encapsulation of furosemide microcrystals for controlled drug release. J. Control. Release. Elsevier; 86 (1), 59_68.
28. Al-Jamal, W., Kostarelos, K., 2007. Liposome--nanoparticle hybrids for multimodal diagnostic and therapeutic applications. Nanomedicine; Future Medicine; 2 (1), 85-98.
29. Alexis, F., et al., 2008. Factors affecting the clearance and biodistribution of polymeric nanoparticles. Mol. Pharm. ACS Publications.; 5 (4), 505-515.
30. Amstad, E., 2011. Triggered release from liposomes through magnetic actuation of iron oxide nanoparticle containing membranes. Nano Lett. ACS Publications; 11 (4), 1664-1670.
31. Basuki, J.S., 2014. A block copolymer-stabilized co-precipitation approach to magnetic iron oxide nanoparticles for potential use as MRI contrast agents. Polym. Chem. Royal Society of Chemistry; 5 (7), 2611_2620.
32. Bothun, G.D., Preiss, M.R., 2011. Bilayer heating in magnetite nanoparticle--liposome dispersions via fluorescence anisotropy. J. Colloid Interface Sci. Elsevier. 357 (1), 70-74.

Research Article

33. Laurent S, Forge D, Port M et al., 2008. Magnetic iron oxide nanoparticles: synthesis, stabilization, vectorization, physicochemical characterizations, and biological applications. Chem. Rev.; 108(6), 2064–2110.

34. Arruebo M, Fern´andez-Pacheco R, Ibarra MR, Santamara J., 2007. Magnetic nanoparticles for drug delivery. Nano Today 2(3), 22–32.

35. Li L, JiangW, Luo K, Song H, Lan F, Wu Y, Gu Z., 2013. Super- paramagnetic iron oxide nanoparticles as MRI contrast agents for non-invasive stem cell labelling and tracking. Theranostics 3, 595–615.